THE JOURNAL OF BIOLOGICAL CHEMISTRY
Vol. 276, No. 49, Issue of December 7, pp. 45522–45529, 2001
Printed in U.S.A.

Mutational Analysis of Baculovirus Capping Enzyme Lef4 Delineates an Autonomous Triphosphatase Domain and Structural Determinants of Divalent Cation Specificity*

Received for publication, August 9, 2001, and in revised form, September 10, 2001
Published, JBC Papers in Press, September 11, 2001, DOI 10.1074/jbc.M107615200

Alexandra Martins and Stewart Shuman‡

From the Molecular Biology Program, Sloan-Kettering Institute, New York, New York 10021

The 464-amino acid baculovirus Lef4 protein is a bifunctional mRNA capping enzyme with triphosphatase and guanylyltransferase activities. The hydrolysis of 5′-triphosphate RNA and free NTPs by Lef4 is dependent on a divalent cation cofactor. RNA triphosphatase activity is optimal at pH 7.5 with either magnesium or manganese, yet NTP hydrolysis at neutral pH is activated only by manganese or cobalt. Here we show that Lef4 possesses an intrinsic magnesium-dependent ATPase with a distinctive alkaline pH optimum and a high K_m for ATP (4 mM). Lef4 contains two conserved sequences, motif A (^{8}IEKEISY^{14}) and motif C (^{180}LEYEF^{184}), which define the fungal/viral/protozoal family of metal-dependent RNA triphosphatases. We find by mutational analysis that Glu^{9}, Glu^{11}, Glu^{181}, and Glu^{183} are essential for phosphohydrolase chemistry and likely comprise the metal-binding site of Lef4. Conservative mutations E9D and E183D abrogate the magnesium-dependent triphosphatase activities of Lef4 and transform it into a strictly manganese-dependent RNA triphosphatase. Limited proteolysis of Lef4 and ensuing COOH-terminal deletion analysis revealed that the NH_2-terminal 236-amino acid segment of Lef4 constitutes an autonomous triphosphatase catalytic domain.

The 5′ m7GpppN cap is a distinctive feature of eukaryotic cellular and viral messenger RNA. Several large DNA viruses encode their own capping enzymes, including poxviruses, African swine fever virus, baculoviruses, and *Chlorella* virus PBCV-1. The DNA virus enzymes catalyze the same series of three reactions as the cellular 5′ processing enzymes, in which the 5′ triphosphate end of the transcript is first hydrolyzed to a diphosphate by RNA triphosphatase, the diphosphate end is then capped with GMP by GTP:RNA guanylyltransferase, and the GpppN cap is methylated by AdoMet:RNA (guanine-N7) methyltransferase (1).

The physical organization of the triphosphatase and guanylyltransferase components of the capping apparatus differs among the DNA virus families. The triphosphatase and guanylyltransferase active sites of the *Autographa californica* baculovirus capping enzyme are located within a single 464-amino acid polypeptide encoded by the *Lef4* gene (Fig. 1) (2–4). The Lef4 protein catalyzes the cleavage of the β-γ phosphoanhydride bond of either triphosphate-terminated RNA or free NTPs. The phosphohydrolase activity of Lef4 depends on a divalent cation cofactor (3, 4). The Lef4 triphosphatase belongs to a newly recognized family of metal-dependent NTPases that embraces the RNA triphosphatase components of the capping enzymes of other DNA viruses (poxviruses, African swine fever virus, *Chlorella* virus) and unicellular eukaryotes such as fungi, microsporidia, and Plasmodia (5–12).[1] The family is defined by the presence of two conserved glutamate-containing motifs (motifs A and C, Fig. 1) and the signature biochemical property of hydrolyzing NTPs to NDPs in the presence of manganese or cobalt (7). Motifs A and C of Lef4 are situated in the NH_2-terminal portion of the enzyme (Fig. 1). The COOH-terminal segment includes the six conserved motifs that comprise the active site of the guanylyltransferase (3, 4, 14, 15). All of the motifs in AcNPV Lef4 are conserved in the capping enzymes from other baculoviruses (Fig. 1) and in the 545-amino acid triphosphatase-guanylyltransferase domain of vaccinia virus capping enzyme (4, 5, 16, 17). In contrast to the baculoviruses and poxviruses, *Chlorella* virus PBCV-1 encodes separate RNA triphosphatase and RNA guanylyltransferase enzymes, which are more closely related to the separately encoded triphosphatase and guanylyltransferase components of the fungal capping apparatus than they are to the enzymes from other DNA viruses (11, 18).

The order of the triphosphatase and guanylyltransferase motifs in the primary structures of baculovirus and vaccinia capping enzymes (H_2N-triphosphatase-guanylyltransferase-COOH) mimics the temporal order of the cap-forming reactions. Are the two enzymatic functions linked in some way structurally? Mutational analyses of the vaccinia D1 protein showed that the triphosphatase and guanylyltransferase active sites are distinct, *i.e.* single glutamate-to-alanine mutations in motifs A and C inactivate the vaccinia triphosphatase but spare the guanylyltransferase, whereas single alanine mutations in the COOH-terminal motifs affect the guanylyltransferase but spare the triphosphatase (6, 17). Similarly, it was found that double glutamate-to-alanine mutations in motifs A and C of baculovirus Lef4 selectively inactivated the triphosphatase (4). However, it remains unclear if the triphosphatase and guanylyltransferase domains of Lef4 or D1 are truly autonomous, *e.g.* as is the case for the bifunctional mammalian capping enzyme. Attempts to produce catalytically active subdomains of the vaccinia capping enzyme have thus far been unsuccessful (6, 16). A goal of the present study was to test whether an autonomous triphosphatase domain exists within baculovirus Lef4.

* This work was supported by National Institutes of Health Grant GM42498. The costs of publication of this article were defrayed in part by the payment of page charges. This article must therefore be hereby marked "*advertisement*" in accordance with 18 U.S.C. Section 1734 solely to indicate this fact.

‡ To whom correspondence should be addressed: Molecular Biology Program, Sloan-Kettering Inst., 1275 York Ave., New York, NY 10021. s-shuman@ski.mskcc.org.

[1] Hausmann, S., Vivares, C. P., and Shuman, S. (2001) *J. Biol. Chem.*, in press.

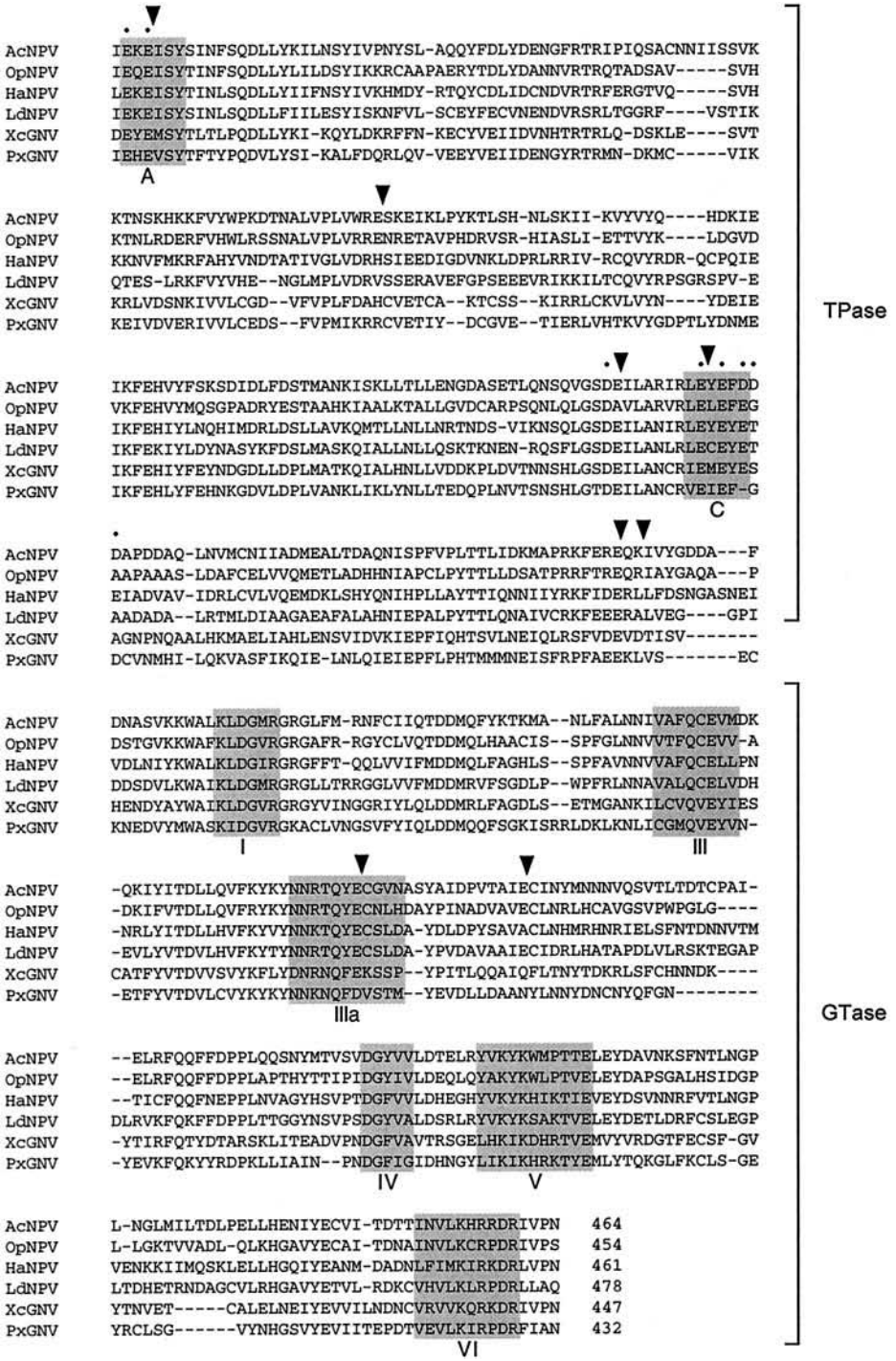

FIG. 1. **Primary structures of baculovirus capping enzymes.** The amino acid sequence of the AcNPV Lef4 protein is aligned to the sequences of the Lef4 homologs from other viruses, including *Orgyia pseudotsugata* nuclear polyhedrosis virus (*OpNPV*), *Heliocoverpa armigera* nuclear polyhedrovirus (*HaNPV*), *Lymantria dispar* nuclear polyhedrosis virus (*LdNPV*), *Xestia c-nigrum granulovirus* (*XcGNV*), and *Plutella xylostella* granulovirus (*PxGNV*). The putative NH_2-terminal triphosphatase (*TPase*) and COOH-terminal guanylyltransferase (*GTase*) domains are denoted in *brackets* on the *right*, and the defining triphosphatase and guanylyltransferase conserved motifs are highlighted in *shaded boxes*. The sites of limited proteolysis of AcNPV Lef4 by V8 and trypsin are denoted by *arrows* above the sequence. Residues mutated in the present study are marked by *dots* above the sequence.

Motifs A and C that define the metal-dependent RNA triphosphatase family consist of alternating glutamate side chains, usually interdigitated with alternating aliphatic/aromatic side chains. In the crystal structure of *Saccharomyces cerevisiae* RNA triphosphatase Cet1, motifs A and C are located within β strands (19). The glutamate side chains of the β strands are pointed into the active site, whereas the hydrophobic side chains of the strands point down into the globular core of the protein. Three of the glutamates directly coordinate the manganese cofactor at the active site and a fourth glutamate coordinates a water molecule bound to the metal (19). This hydrophilic/hydrophobic sequence pattern is reprised in Lef4 motif C and, with some variation, in motif A, suggesting that the structural context for metal binding by Lef4 may be similar to that of Cet1. To test the hypothesis that motifs A and C are involved in metal binding, we subjected the four glutamates of motifs A and C and the aspartates surrounding motif C to alanine scanning and conservative mutational analysis.

A related goal of this effort was to explore the basis for the characteristic activation of NTP hydrolysis by manganese and cobalt, and the apparent inability of Lef4 to hydrolyze NTPs in the presence of magnesium, even though magnesium is perfectly able to activate the RNA triphosphatase function of Lef4 (3, 4). The same divalent cation specificity in NTP hydrolysis is observed for other metal-dependent triphosphatase family members (7, 9–12), with the exception of vaccinia D1, which is activated by magnesium to hydrolyze free NTPs (16, 20). Key questions are as follows: is this capacity truly unique to the

poxvirus enzyme or does it require exceptional reaction conditions not tested previously with Lef4? Are there structural determinants at the active site of Lef4 that dictate selection of the divalent cation cofactor?

MATERIALS AND METHODS

Missense Mutants of LEF-4—Silent diagnostic restriction sites and single alanine or conservative amino acid substitutions were introduced into the *Lef4* gene by PCR[2] using the two-stage overlap extension method. Plasmid pET-LEF4 (4) was the template for the first-stage PCR amplification. The mutated *Lef4* genes were digested with *Nde*I and *Bam*HI and inserted into pET-16b. The inserts were sequenced completely to confirm the presence of the desired substitutions and to ensure that no extra mutations had been acquired during amplification or cloning.

Carboxyl-terminal Truncations of Lef4—Carboxyl-terminal truncation mutants were amplified by PCR using antisense primers that introduced a translation stop codon in lieu of the codons for Trp^{402} or Ile^{237} and a *Bam*HI restriction site immediately downstream of the new stop codons. The 5′ sense primer introduced a *Bam*HI restriction site immediately upstream of the start codon. The wild-type *Lef4* gene was amplified in parallel to introduce a 5′ *Bam*HI site. The PCR products were digested with *Bam*HI and inserted into the *Bam*HI site of the vector pET28-His-Smt3 (a gift from Dr. Chris Lima, Cornell Medical College). The resulting plasmids encode Lef4 polypeptides fused to an NH_2-terminal His_6-tagged Smt3 leader. The truncated proteins were named Lef4-(1–401) and Lef4-(1–236), respectively. The inserts were sequenced completely to confirm the presence of the desired substitutions and to ensure that no extra mutations were introduced during amplification or cloning.

Protein Expression and Purification—The His_{10}-tagged versions of the wild-type and missense mutant Lef4 proteins were expressed in *Escherichia coli* BL21(DE3) and purified by nickel-agarose affinity chromatography as described previously (4). The recombinant His_{10}-Lef4 proteins were recovered in the 200 mM imidazole eluate fractions. The His_6-Smt3-Lef4 proteins were expressed in *E. coli* BL21(DE3) and purified as follows. One-liter cultures of *E. coli* BL21(DE3)/pET28-His-Smt3-Lef4 were grown at 37 °C in LB medium containing 50 μg/ml kanamycin until the A_{600} reached 0.6. The cultures were adjusted to 2% ethanol, chilled on ice for 30 min, and then incubated at 17 °C for 16 h with continuous shaking. The recombinant His_6-Smt3-Lef4 proteins were isolated from the soluble bacterial extracts by nickel-agarose affinity chromatography (4) and recovered in the 50 and 100 mM imidazole eluate fractions. The enzyme preparations were dialyzed against buffer A (50 mM Tris-HCl, pH 8.0, 2 mM dithiothreitol, 2 mM EDTA, 10% glycerol, 0.1% Triton X-100) containing 50 mM NaCl and then concentrated by centrifugal ultrafiltration using Millipore filter units with a 30-kDa cut-off pore size. The protein concentrations were determined by SDS-PAGE analysis of serial dilutions of the Lef4 preparations in parallel with serial dilutions of a BSA standard. The gels were stained with Coomassie Blue, and the staining intensities of the Lef4 and BSA polypeptides were quantitated using a Digital Imaging and Analysis System from Alpha Innotech Corporation.

ATPase Assay—ATPase activity of the Lef4 proteins was determined by measuring the extent of hydrolysis of [γ-^{32}P]ATP in the presence of different metal cofactors. Reaction mixtures (10 μl) contained various amounts of enzyme and either (*a*) 1 mM $MnCl_2$, 50 mM Tris-HCl, pH 7.5, and 0.1 mM [γ-^{32}P]ATP; (*b*) 2 mM $CoCl_2$, 50 mM Tris-HCl, pH 7.5, and 0.1 mM [γ-^{32}P]ATP; or (*c*) 20 mM $MgCl_2$, 50 mM Tris-HCl, pH 9.0, and 2 mM [γ-^{32}P]ATP. The reactions were incubated at 30 °C for 15 min and terminated with 1 M formic acid. Aliquots of the mixtures were spotted onto polyethyleneimine-cellulose TLC plates, which were developed with 0.5 M LiCl, 1 M formic acid. The reaction products were visualized and quantitated by scanning the TLC plates with a FUJIX BAS2000 Bio-Imaging Analyzer.

RNA Triphosphatase Assay—Reaction mixtures (10 μl) containing 50 mM Tris-HCl, pH 7.5, 5 mM dithiothreitol, 1 μM γ-^{32}P-labeled poly(A), either 0.3 mM $MnCl_2$ or 1 mM $MgCl_2$, and varying amounts of Lef4 were incubated at 30 °C for 15 min and then quenched with 1 M formic acid. Aliquots of the mixtures were spotted onto polyethyleneimine-cellulose TLC plates, which were developed with 0.75 M potassium phosphate, pH 4.3. The reaction products were visualized and quantitated by scanning the plates with a phosphorimager. γ-^{32}P-Labeled poly(A) was synthesized as described previously (20).

[2] The abbreviations used are: PCR, polymerase chain reaction; PAGE, polyacrylamide gel electrophoresis.

RESULTS

Effect of pH on the Divalent Cation Specificity of the Lef4 ATPase—Recent studies of vaccinia D1-(1–545) indicated that its divalent cation specificity for ATP hydrolysis was pH-dependent (21). Therefore, we asked whether variations in pH might unmask a latent magnesium-dependent ATPase activity of baculovirus Lef4. We assayed ATP hydrolysis in Tris buffers from pH 4.0 to 9.5 in the presence of 0.1 mM ATP and either 2 mM MnCl, or 2 mM $CoCl_2$, or 20 mM $MgCl_2$ (Fig. 2*A*). Manganese-dependent ATPase was optimal at pH 7.5 to 8.0 and declined at lower or higher pH values. Cobalt-dependent ATPase was optimal at pH 6.5 to 7.5, yet was virtually nil at pH 8.5, where manganese was still quite active. As noted previously, magnesium did not support ATP hydrolysis at neutral pH, the favored range for manganese and cobalt (Fig. 2*A*). The instructive finding was that low levels of magnesium-activated ATP hydrolysis were detected as the pH was increased to 9.0.

Characterization of the Magnesium-dependent ATPase Activity of Lef4—Additional experiments compared the pH profiles of magnesium-dependent ATP hydrolysis at 0.1 mM ATP and 1 mM ATP. We found that the extent of hydrolysis of 1 mM ATP was an order of magnitude higher than 0.1 mM ATP and that the activity with 1 mM ATP again showed a distinctive alkaline pH optimum, with little or no activity at neutral pH (Fig. 2*B*). We then measured ATP hydrolysis at pH 9.0 as a function of magnesium concentration at two concentrations of ATP (1 and 3 mM). Activity with 1 mM ATP was optimal at 10–40 mM magnesium, whereas hydrolysis of 3 mM ATP was optimal at 20–40 mM magnesium. Little or no activity was observed when the magnesium concentration was below the level of input ATP. The salient finding was that the extent of ATP hydrolysis at 3 mM ATP at 20–40 mM magnesium was 3-fold higher than the activity with 1 mM ATP (Fig. 2*C*), suggesting that much higher concentrations of ATP were required for activity in magnesium compared with the other divalent cations.

Kinetic parameters for the manganese- and magnesium-dependent ATPase activities of Lef4 were determined by measuring the extent of $^{32}P_i$ formation as a function of [γ-^{32}P]ATP concentration. Double-reciprocal plots of the data fit well to linear functions (Fig. 2*D*). We calculated a K_m of 0.1 mM ATP and k_{cat} of 13 s^{-1} for manganese-dependent ATP hydrolysis at pH 7.5 and a K_m of 4 mM ATP and k_{cat} of 30 s^{-1} for the magnesium-dependent ATPase at pH 9.0. The K_m for ATP was 40-fold higher with magnesium. These findings make clear that the prior failure to detect a magnesium-dependent ATPase activity of Lef4 stemmed from the choice of suboptimal pH and substrate concentrations for the activity measurements (3, 4).

Alanine Mutations of Motifs A and C—Jin *et al.* (3) showed that double mutants E9A,E11A (motif A) and E181A, E183A (motif C) abolished the RNA triphosphatase and ATPase activities of Lef4 without affecting the guanylyltransferase. The recently reported crystal structure of the *S. cerevisiae* RNA triphosphatase revealed that the glutamates in motif A and motif C comprise the metal-binding site (19). To better evaluate the contributions of the conserved acidic residues to catalysis by Lef4, we replaced Glu^9, Glu^{11}, Glu^{181}, and Glu^{183} individually with alanine. Alanine mutations were also introduced at flanking acidic positions Asp^{172} (conserved in all other Lef4 homologs aligned in Fig. 1), Asp^{185} (conserved as an acidic residue in most of the Lef4 homologs), Asp^{186}, and Asp^{187}. The Lef4-Ala proteins were produced in *E. coli* as His_{10} fusions and purified from soluble bacterial extracts by nickel-agarose chromatography. SDS-PAGE analysis of the nickel-agarose imidazole eluates revealed a predominant 57-kDa polypeptide corresponding to His_{10}-Lef4 (Fig. 3). The guanylyltransferase activity of each of the Lef4 and Lef-Ala preparations was dem-

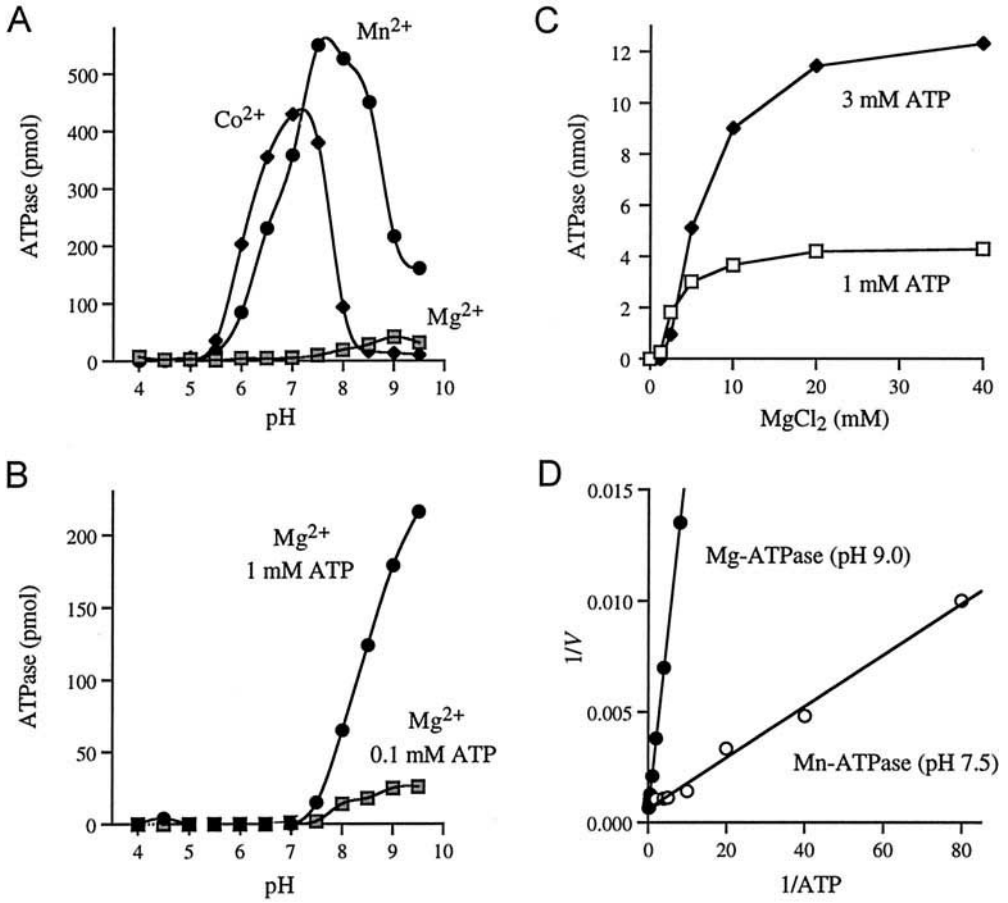

FIG. 2. **Characterization of the metal-dependent ATPase activity of Lef4.** *A*, effect of pH on divalent cation cofactor specificity. ATPase reaction mixtures (10 μl) containing 50 mM buffer: either Tris acetate (pH 4.0, 4.5, 5.0, 5.5, 6.0, 6.5, and 7.0) or Tris-HCl (pH 7.5, 8.0, 8.5, 9.0, and 9.5); 0.1 mM [γ-^{32}P]ATP, 5 ng of Lef4; and either 20 mM $MgCl_2$, 2 mM MnCl or 2 mM $CoCl_2$ were incubated for 15 min at 30 °C. The extent of ATP hydrolysis is plotted as a function of pH. *B*, the pH profile of the magnesium-dependent ATPase activity was determined at 0.1 and 1 mM [γ-^{32}P]ATP. *C*, effect of magnesium concentration. Reaction mixtures contained 50 mM Tris-HCl, pH 9.0, 1 or 3 mM [γ-^{32}P]ATP, 100 ng of Lef4 and $MgCl_2$ as specified. ATPase activity is plotted as function of magnesium concentration. *D*, kinetic analysis. Reaction mixtures (10 μl) containing 5 ng of Lef4, and either (*a*) 50 mM Tris-HCl, pH 7.5, and 2 mM $MnCl_2$, and varying concentrations of [γ-^{32}P]ATP (from 12.5 to 500 μM) or (*b*) 50 mM Tris-HCl, pH 9.0, 20 mM $MgCl_2$, and varying concentrations of [γ-^{32}P]ATP (from 0.125 to 6 mM) were incubated for 15 min at 30 °C. Double-reciprocal plots of the rate of $^{32}P_i$ release (min^{-1} = pmol $^{32}P_i$ formed per 15) *versus* [ATP] (mM^{-1}) are shown.

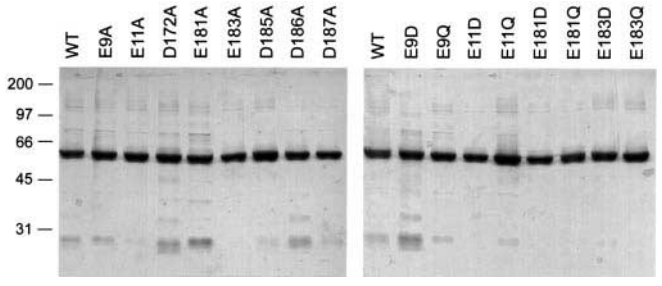

FIG. 3. **Purification of wild-type and mutated versions of Lef4.** Aliquots (1 μg) of the nickel-agarose preparations of wild-type His_{10}-Lef4 (*WT*) and the indicated mutants were analyzed by SDS-PAGE. Polypeptides were visualized by staining with Coomassie Blue dye. The positions (in kilodaltons) of marker proteins are indicated on the *left*. *Left panel*, alanine mutants. *Right panel*, conservative substitution mutants.

onstrated by label transfer from [α-^{32}P]GTP to the enzyme to form a covalent enzyme-GMP adduct (data not shown). That the mutant enzymes retained guanylyltransferase activity indicated that the alanine mutations did not affect the global folding of the Lef4 protein.

The RNA triphosphatase activities of the Lef4 and Lef4-Ala preparations were assayed by the release of $^{32}P_i$ from γ-^{32}P-labeled poly(A) during a 15-min incubation at pH 7.5 in the presence of 1 mM magnesium or 0.3 mM manganese (the optimal pH and metal concentrations for the Lef4 RNA triphosphatase). The specific activities of the Lef4-Ala mutants were normalized to that of the wild-type enzyme and are shown in Table I. The salient findings were that: (i) the E9A and E11A mutations in motif A and the E181A mutation in motif C abrogated RNA triphosphatase activity with either magnesium or manganese as the cofactor (≤0.1% of wild-type specific activity); (ii) the E183A change in motif C abolished magnesium-dependent RNA triphosphatase activity, but the E183A mutant retained 4% residual activity in the presence of manganese; (iii) the D185A, D186A, and D187A mutants were as active as wild-type RNA triphosphatase with either magnesium or manganese; and (iv) the D172A mutant was 3–4-fold more active than wild-type RNA triphosphatase.

The ATPase specific activities were determined with three different divalent cation cofactors at their respective pH optima, and the activities were normalized to that of wild-type Lef4. The mutational effects on ATPase mirrored those observed for the RNA triphosphatase, to wit: (i) mutants E9A, E11A, E181A, and E183A were grossly defective in ATP hydrolysis with manganese, cobalt, and magnesium; (ii) mutants D172A, D185A, D186A, and D187A were at least as active as wild-type Lef4 (Table I).

These results extend the work of Jin *et al.* (3) and establish that each of the four conserved glutamates in motifs A and C is

TABLE I

Mutational effects on the phosphohydrolase activity of Lef4

The purified wild-type and mutant Lef4 proteins were titrated for ATPase activity in reaction mixtures (10 μl) containing either: (*a*) 1 mM $MnCl_2$, 50 mM Tris-HCl, pH 7.5, and 0.1 mM [γ-^{32}P]ATP; (*b*) 2 mM $CoCl_2$, 50 mM Tris-HCl, pH 7.5, and 0.1 mM [γ-^{32}P]ATP; or (*c*) 20 mM $MgCl_2$, 50 mM Tris-HCl, pH 9.0, and 2 mM [γ-^{32}P]ATP. The proteins were titrated for RNA triphosphatase activity in reaction mixtures (10 μl) containing 50 mM Tris-HCl, pH 7.5, 5 mM dithiothreitol, 1 μM γ-^{32}P-labeled poly(A), and either 0.3 mM $MnCl_2$ or 1 mM $MgCl_2$. All reaction mixtures were incubated for 15 min at 30 °C. ATPase and RNA triphosphatase specific activities were determined in the linear range of protein dependence and are expressed as percentages of the specific activity of wild-type Lef4. Each value is the average of at least two independent titration experiments. The ATPase turnover numbers for wild-type Lef4 were 8 s^{-1} for manganese, 5 s^{-1} for cobalt, and 4 s^{-1} for magnesium. The RNA triphosphatase turnover numbers were 30 min^{-1} for manganese and 23 min^{-1} for magnesium.

Lef4 mutant	ATPase			RNA Triphosphatase	
	$MnCl_2$	$CoCl_2$	$MgCl_2$	$MnCl_2$	$MgCl_2$
	% of WT			*% of WT*	
E9A	<0.1	0.1	0.4	0.1	<0.1
E9D	16	11	1.2	48	1
E9Q	<0.1	<0.1	0.7	0.1	<0.1
E11A	<0.1	<0.1	0.4	<0.1	<0.1
E11D	<0.1	<0.1	0.1	0.9	0.1
E11Q	<0.1	<0.1	0.4	0.2	0.1
D172A	95	96	130	300	410
E181A	0.4	<0.1	0.4	0.1	0.1
E181D	7	0.9	1.9	21	0.3
E181Q	<0.1	<0.1	0.7	0.5	0.1
E183A	0.9	0.6	0.6	4	0.1
E183D	76	56	140	130	100
E183Q	4	1	0.9	12	0.3
D185A	140	180	110	140	130
D186A	190	310	190	140	230
D187A	220	330	140	60	140

essential for Lef4 phosphohydrolase activity. The glutamate mutational effects are specific, insofar as alanine substitutions for four other neighboring carboxylate side chains were without deleterious effect on Lef4 activity.

Effects of Conservative Mutations on Lef4 Triphosphatase Activity—The four essential glutamates were substituted conservatively by aspartate and glutamine. The E9D, E9Q, E11D, E11Q, E181D, E181Q, E183D, and E183Q proteins were produced in *E. coli* as His_{10} fusions and purified from soluble bacterial extracts by nickel-agarose column chromatography (Fig. 3). Their RNA triphosphatase and ATPase specific activities (expressed as the percent of the wild-type specific activity) are shown in Table I.

The expectation is that if an essential glutamate side chain is directly coordinating the metal cofactor via electrostatic interactions, then replacement of glutamate by glutamine would not restore triphosphatase activity above the residual level catalyzed the glutamate-to-alanine mutant. Whether an aspartate (which has a shorter distance from main chain to carboxylate) will restore activity depends on how well the "retracted" carboxylate can be accommodated within the coordination sphere of the metal cofactor.

These heuristic points are illustrated by the contrasting effects of conservative mutations in the glutamates of motif A (Table I). We found that the E11D and E11Q mutants were defective in their RNA triphosphatase and ATPase functions with all of the metal cofactors tested. Thus, we construe that: (i) Glu^{11} is likely to coordinate the divalent metal directly, and (ii) the enzyme cannot flex its structure to bring an aspartate into the metal coordination sphere. Replacing Glu^{9} with glutamine also resulted in a gross catalytic defect with all of the metals, but the E9D mutant was selectively defective in magnesium-dependent phosphohydrolase function, with both RNA and free NTP substrates. Remarkably, the introduction of aspartate restored manganese-dependent RNA triphosphatase to 48% of the wild-type activity and partially restored manganese-dependent and cobalt-dependent ATPase to 16 and 11% of the respective wild-type levels. This represents a substantial gain-of-function compared with the activities of the E9A mutant. We surmise that: (i) Glu^{9} likely interacts directly with the metal cofactor, (ii) the enzyme can accommodate Asp9 in the metal coordination sphere, and (iii) the E9D mutation dramatically alters the divalent cation specificity of the Lef4 RNA triphosphatase. Possible explanations for this effect will be discussed.

In motif C, the E181Q change did not revive triphosphatase activity with either RNA or free nucleotide. However, the E181D substitution restored significant manganese-dependent RNA triphosphatase (21% of wild-type Lef4 activity) while failing to hydrolyze the RNA substrate in the presence of magnesium (0.3% activity) (Table I). The E181D mutation also elicited a modest but significant gain-of-function in manganese-dependent ATP hydrolysis, with little salutary effect on cobalt-dependent and magnesium-dependent ATPase. The enzyme could apparently accommodate manganese, but not cobalt or magnesium.

Changing Glu^{183} to glutamine resulted in 3–4-fold gains of activity in manganese-dependent RNA triphosphatase and manganese-dependent ATPase activities compared with the level of the E183A mutant (Table I). The striking finding was that introduction of aspartate restored activity across the board to wild-type or near wild-type levels. Thus, the enzyme easily accommodated the shortened linker arm of the aspartate side chain.

Probing Lef4 Structure by Limited Proteolysis—Recombinant His_{10}-Lef4 was subjected to proteolysis with increasing amounts of trypsin and V8 proteases. NH_2-terminal sequencing of the undigested polypeptide by automated Edman chemistry after transfer from an SDS gel to a polyvinylidene difluoride membrane confirmed that the NH_2-terminal sequence (GHHHHH) corresponded to that of the recombinant gene product starting from the second residue of the His-tag (Fig. 4*A*). Apparently, the capping enzyme suffered removal of the initiating methionine during expression in *E. coli*. Scission of Lef4 by trypsin yielded two major products that were stable at

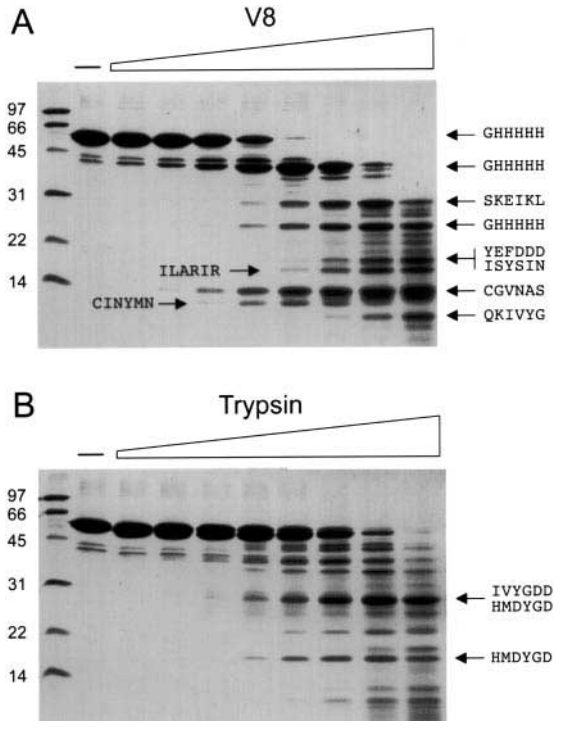

FIG. 4. **Limited proteolysis of Lef4.** Reaction mixtures (10 μl) containing 50 mM Tris-HCl, pH 8.0, and 6 μg of His_{10}-Lef4 were incubated with increasing amounts (0.1, 0.3, 1, 3, 10, 30, 100, or 300 ng) of either V8 protease (*A*) or trypsin (*B*) for 10 min at 22 °C. Control samples contained no protease (−). The reactions were quenched with 1% SDS, and the digests were analyzed by SDS-PAGE. The proteolysis products were visualized by staining with Coomassie Blue dye. The positions and sizes (in kilodaltons) of marker proteins are indicated on the *left*. A parallel set of digests was resolved by SDS-PAGE, transferred to a polyvinylidene difluoride membrane, and the indicated polypeptide bands were subjected to automated NH_2-terminal sequencing (13). The NH_2-terminal sequences are denoted in single-letter code.

levels of trypsin sufficient to cleavage all of the input Lef4: (i) a ~16-kDa species (sequence HMDGYD) resulting from tryptic cleavage of the His-tag 2 residues upstream of Met^1 of the Lef4 protein, and (ii) a mixture of two tryptic products migrating at ~27 kDa, one of which (sequence IVYGDD) resulted from cleavage between Lys^{236} and Ile^{237} and a second fragment (sequence HMDGYD) originating from the N terminus of Lef4 absent the His-tag (Fig. 4*B*). The Lys^{236}-Ile^{237} cleavage site, denoted by an *arrow* above the Lef4 sequence in Fig. 1, is located downstream of triphosphate motif C and upstream of guanylyltransferase motif I.

Treatment of Lef4 with V8 protease yielded multiple products that were resistant to digestion by V8 concentrations sufficient to cleavage all of the input Lef4 (Fig. 4*A*). Initial scission at limiting V8 concentration produced an ~40-kDa species that retained the original NH_2 terminus of the His-tag (GHHHHH) and a ~14-kDa species (sequence CGVNAS) arising from cleavage between Glu^{326} and Cys^{327}. The Glu^{326}-Cys^{327} cleavage site is conserved in other Lef4 homologs and is located within guanylyltransferase motif IIIa (see Fig. 1). Also arising at limiting V8 concentrations was a minor ~12-kDa species (sequence CINYMN) generated by cleavage between Glu^{332} and Cys^{343}; this site is located just downstream of guanylyltransferase motif IIIa (Fig. 1). At higher V8 concentrations, the ~40-kDa species decayed and gave rise to an ~24-kDa fragment that retained the NH_2-terminal His-tag plus a ~27-kDa species (sequence SKEIKL) arising from scission between Glu^{94} and Ser^{95}. This site is located between triphosphatase motifs A and C within a segment of Lef4 that is not well conserved in other viral homologs. Thus, the Glu^{94}-Ser^{95} dipeptide may demarcate a surface accessible loop within a putative triphosphatase domain. At the highest levels of V8, there appeared three new protease-resistant fragments. A ~17-kDa band contained a mixture of two species, one (sequence YEFDDD) arising from cleavage between Glu^{181} and Tyr^{182} within triphosphatase motif C and a second (sequence ISYSIN) generated by cleavage between Glu^{11} and Ile^{12} in triphosphatase motif A (Fig. 1). This finding is remarkable in light of previous studies showing that the principal sites of V8 accessibility in the vaccinia triphosphatase-guanylyltransferase also mapped to the glutamates within motif A and C (6). A ~16-kDa fragment (sequence ILARIR) was formed by scission between Glu^{173} and Ile^{174}, just upstream of motif C (Fig. 1). A small (~10 kDa) fragment produced at the highest V8 concentration (sequence QKIVYG) resulted from scission between Glu^{234} and Gln^{235} (Fig. 4*A*). The Glu^{234}-Gln^{235} V8 site is immediately vicinal to the Lys^{236}-Ile^{237} tryptic cleavage site (Fig. 1). This protease-sensitive segment between the triphosphatase and guanylyltransferase motifs may therefore demarcate an interdomain linker.

Deletion Analysis of Lef4 Defines an Autonomous Triphosphatase Domain—To determine whether the NH_2 terminus of Lef4 comprises an autonomous triphosphatase domain, we engineered two COOH-terminal deletion mutants, Lef4-(1–401) and Lef4-(1–236). The Lef4-(1–401) derivative is truncated within guanylyltransferase motif V. Crystallographic analysis of *Chlorella* virus guanylyltransferase revealed that the protein consists of two structural domains separated by an interdomain cleft (14). The larger NH_2-terminal domain includes motifs I, III, IIIa, and IV, whereas the COOH-terminal domain includes motif VI. Motif V resides within a flexible β strand that links the two folded domains. Thus, we chose to truncate Lef4 after residue 401, which demarcates the boundary between the two guanylyltransferase structural domains in the *Chlorella* virus protein. The Lef4-(1–236) derivative is truncated at the trypsin-accessible site that we suggested might represent a boundary between putative triphosphatase and guanylyltransferase functional domains. Recombinant Lef4, Lef4-(1–401), and Lef4-(1–236) were produced in bacteria as NH_2-terminal His_6-Smt3 fusions (22) and then purified from soluble bacterial lysates by nickel-agarose chromatography (Fig. 5). The use of the His_6-Smt3 fusion system improved the solubility of the truncated recombinant Lef4 proteins. His_6-Smt3-Lef4 migrated more slowly than His_{10}-Lef4 during SDS-PAGE, as expected from the larger size of the His_6-Smt3 leader. The truncated versions migrated more rapidly during SDS-PAGE, as expected.

The recombinant proteins were assayed for manganese-dependent ATPase activity. Control titrations showed that the specific activity of the His_6-Smt3-Lef4 protein was 90% of the activity of His_{10}-Lef4, indicating that the His_6-Smt3 tag did not adversely affect Lef4 function. Lef4-(1–401) was just as active as full-length Lef4 in manganese-dependent ATP hydrolysis (Fig. 5), but was completely inert in enzyme-GMP adduct formation (not shown). We conclude that the COOH-terminal structural component of the guanylyltransferase domain does not include any residues involved in phosphohydrolase reaction chemistry. The more instructive finding was that Lef4-(1–236), which includes none of the guanylyltransferase motifs, retained nearly half of the of the wild-type triphosphatase activity (Fig. 5). ATP hydrolysis by Lef4-(1–236) was completely dependent on a divalent cation cofactor (not shown). We constructed and purified a mutated version of Lef4-(1–236) in which Glu^{11} in motif A was replaced by alanine. The E11A change completely abrogated the manganese-dependent ATPase of the truncated Lef4-(1–236) protein (Fig. 5).

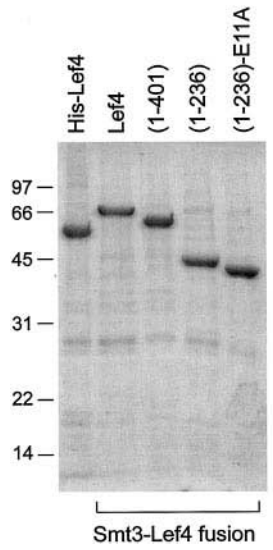

Smt3-Lef4 protein	Mn·ATPase (k_{cat}, % of WT)
Lef4	100
(1-401)	100
(1-236)	43
(1-236) E11A	<0.1

FIG. 5. **Autonomous NH_2-terminal triphosphatase domain of Lef4.** Aliquots (1 μg) of wild-type His_{10}-Lef4 and the indicated His_6-Smt3-Lef4 fusion proteins were analyzed by SDS-PAGE. The Coomassie Blue-stained gel is shown. The Lef4 proteins were titrated for manganese-dependent ATPase activity in reaction mixtures (10 μl) containing 50 mM Tris-HCl, pH 7.5, 1 mM $MnCl_2$, and 0.1 mM [γ-^{32}P]ATP. The reaction mixtures were incubated for 15 min 30 °C. The specific activities were determined in the linear range of protein dependence and are expressed as the percentage of the specific activity of wild-type His_6-Smt3-Lef4 (turnover number 7 s^{-1}). Each value is the average of at least two independent titration experiments.

We conclude that the 236-amino acid NH_2-terminal fragment of Lef4 defined by limited digestion with trypsin comprises a fully autonomous metal-dependent triphosphatase domain. This is the first instance in which an autonomous triphosphatase domain has been delineated within a bifunctional viral triphosphatase-guanylyltransferase enzyme.

DISCUSSION

Baculovirus Lef4 and vaccinia virus D1-(1–545) are bifunctional triphosphatase-guanylyltransferase enzymes that catalyze the first two steps of mRNA cap formation. Both viral proteins contain the signature triphosphatase and guanylyltransferase motifs, which are arrayed in the order H_2N-triphosphatase-guanylyltransferase-COOH. A similar organization of the catalytic motifs is seen in the bifunctional triphosphatase-guanylyltransferase enzyme encoded by the *Kluyveromyces lactis* cytoplasmic linear DNA plasmid pGKL2 (23). Although the triphosphatase and guanylyltransferase enzymes of fungi and *Chlorella* virus contain the same constellations of catalytic motifs, the component activities reside on separate polypeptides. Whereas efforts to partition the vaccinia capping enzyme into triphosphatase and guanylyltransferase domains have not met with success, we show here that the NH_2-terminal 236-amino acid segment of baculovirus Lef4 constitutes a "stand-alone" metal-dependent phosphohydrolase domain.

The Lef4 triphosphatase domain boundary is demarcated within native Lef4 by closely spaced sites of accessibility to trypsin and V8 proteases, consistent with the existence of a flexible interdomain linker or a surface-exposed interdomain loop. Treatment of vaccinia D1-(1–545) with V8 did not result in cleavage between triphosphatase motif C and guanylyltransferase motif I (this interval in the D1 polypeptide contains four potential sites for V8 cleavage at glutamate); rather the principal V8-sensitive sites in D1 were located at the second glutamate in motif A at the first glutamate in motif C (6). We found that the same sites were cleaved during V8 proteolysis of Lef4. Therefore, we surmise that the metal-binding sites of the baculovirus and vaccinia triphosphatases are likely to be exposed on the protein surface, rather than enclosed within a tunnel, as it is in the yeast RNA triphosphatase Cet1 (19).

Mutational analysis of Lef4 motifs A and C provides strong evidence that Glu^9, Glu^{11}, Glu^{181}, and Glu^{183} are the constituents of the metal-binding site of the triphosphatase. Because glutamine substitutions at positions 9, 11, and 181 reduced RNA triphosphatase and ATPase activity by at least 2 orders of magnitude, we suspect that Glu^9, Glu^{11}, and Glu^{181} coordinate directly to the metal cofactor via a "hard" ionic interaction (24). The E183Q mutant displays a low but significant residual manganese-dependent RNA triphosphatase activity (12% of wild-type), which may signify that: (i) direct interaction between manganese and the side chain carbonyl of glutamine supports this residual activity or (ii) the side chain at position 183 coordinates the metal indirectly through a water molecule. The effects of Glu-to-Gln changes on Lef4 triphosphatase activity are consistent with the effects reported previously for the motif A and C residues of vaccinia D1-(1–545), *i.e.* glutamines were not tolerated at either Glu^{37}, Glu^{39}, or Glu^{192} of the vaccinia triphosphatase, but the E194Q mutant retained 80% of the wild-type RNA triphosphatase activity (21). The crystal structure of yeast RNA triphosphatase shows that three of the four glutamates coordinate manganese directly (*i.e.* both glutamates in motif A and the distal glutamate in motif C), whereas the fourth glutamate interacts with a water molecule in the octahedral coordination complex of the manganese ion (19). Perhaps the direct *versus* indirect metal-binding modes of the motif C glutamates have been inverted in the baculovirus and vaccinia RNA triphosphatases compared with the yeast enzyme.

The most striking outcome of the mutational analysis was the change in metal cofactor specificity elicited by the E9D and E181D mutations. These conservative substitutions ablated the magnesium-dependent phosphohydrolase activities of Lef4 and transformed it into a strictly manganese-dependent RNA triphosphatase. A plausible interpretation of the altered metal specificity is that introduction of the shorter aspartate side chain makes Lef4 acutely sensitive to the atomic radius of the available divalent metal ion cofactor. The atomic radius of Mg(II) with a coordination number of 6 is 0.65 Å, whereas the radius of Co(II) is 0.70 Å, and the radius of Mn(II) is 0.80 Å (24). Thus, an aspartate at position 9 or position 181 might be able to access the coordination complex with manganese, because manganese has the longest atomic radius, whereas Asp^9 would not reach the coordination complex of magnesium, which has the shortest radius. Cobalt, with its intermediate atomic radius, appears to accommodate the aspartate at position 9 to effect ATP hydrolysis, but not the aspartate at position 181. The abrogation of triphosphatase activity with all metal cofactors by the E11D mutation implies that the shorter side chain cannot reach even the largest of the three metal coordination spheres. On the other hand, the robust activity of the E183D mutant suggests there is little difficulty in placing the shorter carboxylate (directly or indirectly) in the metal coordination complex. This easy accommodation may reflect flexibility of the main chain, or it may indicate that the natural Glu^{183} side chain is not in a fully extended conformation when it binds either to the metal or to a metal-bound water. Delineation of the geometry of the metal-binding site of the baculovirus capping enzyme and the tertiary structure of its active site will hinge on obtaining a crystal structure of either the complete Lef4 protein or the autonomous NH_2-terminal triphosphatase domain identified presently.

REFERENCES

1. Shuman, S. (2000) *Prog. Nucleic Acids Res. Mol. Biol.* **66,** 1–40
2. Guarino, L. A., Jin, J., and Dong, W. (1998) *J. Virol.* **72,** 10003–10010
3. Jin, J., Dong, W., and Guarino, L. A. (1998) *J. Virol.* **72,** 10011–10019
4. Gross, C. H., and Shuman, S. (1998) *J. Virol.* **72,** 10020–10028
5. Yu, L., and Shuman, S. (1996) *J. Virol.* **70,** 6162–6168
6. Yu, L., Martins, A., Deng, L., and Shuman, S. (1997) *J. Virol.* **71,** 9837–9843
7. Ho, C. K., Pei, Y., and Shuman, S. (1998) *J. Biol. Chem.* **273,** 34151–34156
8. Pei, Y., Ho, C. K., Schwer, B., and Shuman, S. (1999) *J. Biol. Chem.* **274,** 28865–28874
9. Pei, Y., Lehman, K., Tian, L., and Shuman, S. (2000) *Nucleic Acids Res.* **28,** 1885–1892
10. Pei, Y., Schwer, B., Hausmann, S., and Shuman, S. (2001) *Nucleic Acids Res.* **29,** 387–396
11. Ho, C. K., Gong, C., and Shuman, S. (2001) *J. Virol.* **75,** 1744–1750
12. Ho, C. K., and Shuman, S. (2001) *Proc. Natl. Acad. Sci. U. S. A.* **98,** 3050–3055
13. Sekiguchi, J., and Shuman, S. (1997) *Nucleic Acids Res.* **25,** 727–734
14. Håkansson, K., Doherty, A. J., Shuman, S., and Wigley, D. B. (1997) *Cell* **89,** 545–553
15. Wang, S. P., Deng, L., Ho, C. K., and Shuman, S. (1997) *Proc. Natl. Acad. Sci. U. S. A.* **94,** 9573–9578
16. Myette, J. R., and Niles, E. G. (1996) *J. Biol. Chem.* **271,** 11936–11944
17. Cong. P., and Shuman, S. (1995) *Mol. Cell. Biol.* **15,** 6222–6231
18. Ho, C. K., Van Etten, J. L., and Shuman, S. (1996) *J. Virol.* **70,** 6658–6664
19. Lima, C. D., Wang, L. K., and Shuman, S. (1999) *Cell* **99,** 533–543
20. Shuman, S., Surks, M., Furneaux, H., and Hurwitz, J. (1980) *J. Biol. Chem.* **255,** 11588–11598
21. Ho, C. K., Martins, A., and Shuman, S. (2000) *J. Virol.* **74,** 5486–5494
22. Mossessova, E., and Lima, C. D. (2000) *Mol. Cell* **5,** 865–876
23. Tiggemann, M., Jeske, S., Larsen, M., and Meinhardt, F. (2001) *Yeast* **18,** 815–825
24. Glusker, J. P. (1991) *Adv. Protein Chem.* **42,** 1–76